
Empowering Pre-Trained Language Models for Spatio-Temporal Forecasting via Decoupling Enhanced Discrete Reprogramming

Hao Wang¹, Jindong Han², Wei Fan³, Hao Liu^{1,2}

¹The Kong Kong University of Science and Technology (Guangzhou)

²The Kong Kong University of Science and Technology

³University of Oxford

hwang574@connect.hkust-gz.edu.cn, jhanao@connect.ust.hk
wei.fan@wrh.ox.ac.uk, liuh@ust.hk

Abstract

Spatio-temporal time series forecasting plays a critical role in various real-world applications, such as transportation optimization, energy management, and climate analysis. The recent advancements in Pre-trained Language Models (PLMs) have inspired efforts to reprogram these models for time series forecasting tasks, by leveraging their superior reasoning and generalization capabilities. However, existing approaches fall short in handling complex spatial inter-series dependencies and intrinsic intra-series frequency components, limiting their spatio-temporal forecasting performance. Moreover, the linear mapping of continuous time series to a compressed subset vocabulary in reprogramming constrains the spatio-temporal semantic expressivity of PLMs and may lead to potential information bottleneck. To overcome the above limitations, we propose REPST, a tailored PLM reprogramming framework for spatio-temporal forecasting. The key insight of REPST is to decouple the spatio-temporal dynamics in the frequency domain, allowing better alignment with the PLM text space. Specifically, we first decouple spatio-temporal data in Fourier space and devise a structural diffusion operator to obtain temporal intrinsic and spatial diffusion signals, making the dynamics more comprehensible and predictable for PLMs. To avoid information bottleneck from a limited vocabulary, we further propose a discrete reprogramming strategy that selects relevant discrete textual information from an expanded vocabulary space in a differentiable manner. Extensive experiments on four real-world datasets show that our proposed approach significantly outperforms state-of-the-art spatio-temporal forecasting models, particularly in data-scarce scenarios.

1 Introduction

Spatio-temporal time series forecasting aims to predict future states of real-world complex systems by simultaneously learning spatial and temporal dependencies of historical observations, which plays a pivotal role in diverse real-world applications, such as traffic management [21, 37], environmental monitoring [12], and resource optimization [6]. In recent years, deep learning has demonstrated great predictive power and led to a surge in deep spatio-temporal forecasting models [38, 16]. For example, Recurrent Neural Networks (RNNs) and Graph Neural Networks (GNNs) are widely leveraged to capture complex spatio-temporal patterns [16]. Despite fruitful progress, existing approaches are typically limited to the one-task-one-model setting, which lacks general-purpose utility and inevitably falls short in handling practical data-scarce scenarios, *e.g.*, newly deployed monitoring services.

In recent years, we have witnessed the breakthrough of Pre-trained Language Models (PLMs) in the Natural Language Processing (NLP) domain, such as GPT-3 [2] and LLaMA [36]. PLMs exhibit outstanding contextual understanding, reasoning, and few-shot capabilities on a broad range of tasks by pre-training on extensive text corpora. Although initially designated to deal with textual data, the impressive capabilities of PLMs have inspired their application to time series [46, 17, 18]. FPT [46] pioneers research in this direction and showcases the promise of fine-tuning PLMs as generic time series feature extractors, but it overlooks the modality divergence between time series and natural language, which may limit the PLM potentials. To address this issue, model reprogramming [17, 18] adapts time series data into textual representations that are understandable by language models. For example, Time-LLM [17] reprograms PLMs for solving time series forecasting tasks by learning an input transformation function that maps time series patches [30] to a small compressed vocabulary. Such a method offers a promising solution to fully unlock the predictive capabilities of PLMs.

However, two major challenges prevent the application of existing reprogramming methods to spatio-temporal time series forecasting. The first challenge is the intricate nature of spatio-temporal signals, which encompass both intrinsic temporal components and latent spatial diffusion components [33, 5]. Capturing these fine-grained spatio-temporal dynamics in natural language through direct reprogramming of raw signals can result in inefficient information utilization. The second challenge lies in cross-modality data alignment. Existing reprogramming approaches, such as Time-LLM, use a compressed vocabulary that may not be expressive enough to encode complex spatio-temporal semantics. Simply expanding the vocabulary increases the search space and poses a risk of overfitting due to the combinatorial nature of discrete words.

To this end, in this paper, we introduce a spatio-temporal reprogramming block that aligns spatio-temporal time series with the PLMs' embedding space, unlocking their capabilities to comprehend sophisticated spatio-temporal patterns. Specifically, we first construct a spatio-temporal decoupling block that combines Fourier analysis and structural diffusion operator, for decomposing input spatio-temporal data into intrinsic and diffusive components, respectively. These disentangled components enable PLMs to better understand diverged spatio-temporal patterns within the text space. Furthermore, we propose a discrete reprogramming strategy that efficiently extracts the most relevant word tokens from the complete vocabulary of PLMs in a differentiable manner through reparameterization. This approach expands the reprogramming space while mitigating the risk of overfitting, ensuring robust and accurate spatio-temporal forecasting.

Based on the proposed block, we construct REPST, a reprogrammed PLM framework tailored to spatio-temporal forecasting tasks. The REPST framework consists of three components: (1) a spatio-temporal reprogramming block, (2) a frozen PLM, and (3) a learnable mapping function between textual representations and desired target outputs. We evaluate REPST on various spatio-temporal forecasting tasks, *i.e.*, energy management, air quality prediction and traffic forecasting. Extensive experimental results show the promising power of the proposed approach compared to state-of-the-art spatio-temporal forecasting models, especially under few-shot scenarios. Our major contributions can be summarized as follows:

- We propose a spatio-temporal reprogramming block, which aligns spatio-temporal data with the text space of language models. The proposed block reduces the difficulty of cross-modality data alignment by disentangling input signals into more interpretable components.
- We further construct REPST, a spatio-temporal forecasting framework that empowers PLM to comprehend complex spatio-temporal patterns through reprogramming. The reprogramming module is optimized in an end-to-end differentiable manner that allows the pre-trained language model to generate desired spatio-temporal predictions without altering any parameters.
- Compared with state-of-the-art baseline methods, the proposed REPST achieves consistent performance improvements on four real-world datasets in three different domains and demonstrates strong few-shot generalization abilities in data-scarce scenarios.

2 Preliminaries

In this section, we introduce some basic notations and formally define the spatio-temporal forecasting problem we aim to address.

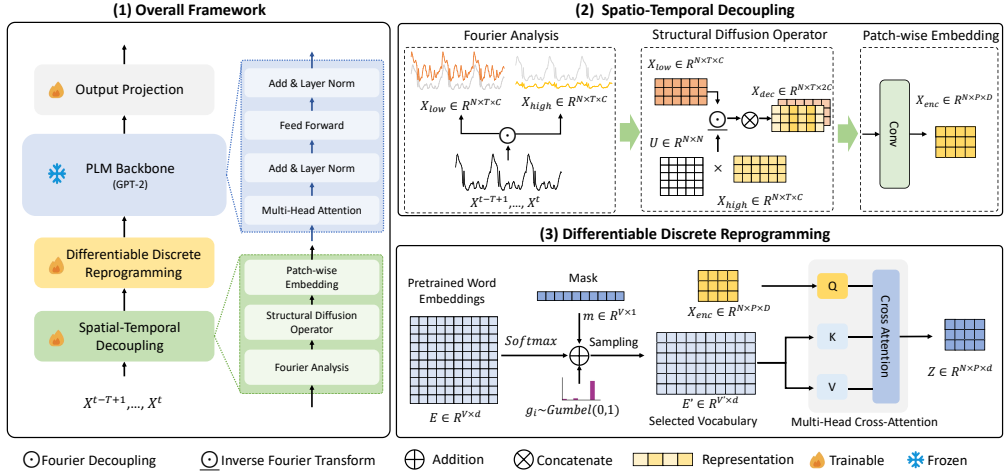


Figure 1: The model framework of REPST. (1) Given a raw input spatio-temporal series, we first decouple the series in Fourier Space and perform structural diffusion. (2) After that, the processed series of each node is divided into patches and further transformed into embeddings by a convolution layer. (3) Then, these patch embeddings are aligned with natural languages by reprogramming with reconstructed pre-trained word embeddings of GPT-2 and further processed by our frozen GPT-2 backbone. The output patches of the pre-trained language model are reprocessed by a learnable mapping function to generate the forecasts.

Consider a set of N nodes \mathcal{V} , where each node in \mathcal{V} corresponds to an entity (e.g., grids, regions, and sensors) in spatial-temporal forecasting scenarios. We denote $\mathbf{x}_{t-T+1:t}^i = [\mathbf{x}_{t-T+1}^i, \mathbf{x}_{t-T}^i, \dots, \mathbf{x}_t^i]^\top \in \mathbb{R}^{T \times C}$ as the observations of node i from time step $t - T + 1$ to t , where T and C represents the look-back window length and the number of time-varying features, such as traffic states and weather conditions. The goal of spatio-temporal forecasting problem is to predict future states for all nodes $i \in \mathcal{V}$ over the next τ time steps based on historical observations:

$$\hat{\mathbf{Y}}_{t+1:t+\tau} = f_\theta(\mathbf{X}_{t-T+1:t}), \quad (1)$$

where $\mathbf{X}_{t-T+1:t} = [\mathbf{x}_{t-T+1:t}^0, \mathbf{x}_{t-T+1:t}^1, \dots, \mathbf{x}_{t-T+1:t}^{N-1}]^\top \in \mathbb{R}^{N \times T \times C}$ denotes the history data input in previous T time steps, and f_θ is the spatio-temporal forecasting model parameterized by θ .

$\hat{\mathbf{Y}}_{t+1:t+\tau} = \{\hat{\mathbf{y}}_{t+1:t+\tau}^i\}_{i=0}^N$ and $\mathbf{Y}_{t+1:t+\tau} = \{\mathbf{y}_{t+1:t+\tau}^i\}_{i=0}^N$ denote the estimated future states and the ground truth in the next τ time steps, where $\hat{\mathbf{Y}}_{t+1:t+\tau}, \mathbf{Y}_{t+1:t+\tau} \in \mathbb{R}^{N \times \tau \times C}$. For convenience, we omit the lower corner mark and represent $\mathbf{X}_{t-T+1:t}, \mathbf{Y}_{t+1:t+\tau}$ as \mathbf{X}, \mathbf{Y} and $\mathbf{x}_{t-T+1:t}^i, \mathbf{y}_{t+1:t+\tau}^i$ as $\mathbf{x}^i, \mathbf{y}^i$. Furthermore, we denote the representation of any variable λ in Fourier space as $\hat{\lambda}$.

3 Methodology

As illustrated in Figure 1, REPST consists of three components: a spatio-temporal reprogramming block, a frozen Pre-trained Language Model (PLM), and a learnable output mapping layer. To be specific, in spatio-temporal reprogramming block, we first decompose the input signals in Fourier space and diffuse the high-frequency signals based on a pre-defined spatial topology structure. Then we utilize a differentiable discrete sampling strategy to build the relationship between the decoupled signals and text modality. After that, we employ a frozen PLM to obtain spatio-temporal representations for each node. Finally, a learnable mapping function generates future predictions based on the representations of PLM. We will introduce each component of REPST in detail below.

3.1 Spatio-Temporal Reprogramming

Recent studies have revealed that PLMs possess rich spatio-temporal knowledge and reasoning capabilities [10, 29, 18]. Regardless, PLMs showcase proficient language understanding and processing skills, but inherently lack an in-depth comprehension of intricate spatio-temporal patterns hidden in numerical data as they are not included in the pre-training dataset. In this section, we address the divergence between these two modalities through a carefully designed reprogramming module, making PLMs more easily to perform spatio-temporal forecasting tasks.

Spatio-Temporal Decoupling. As aforementioned, language models face difficulties in comprehending the hybrid dynamics of spatio-temporal signals, which encompasses evolving patterns over both space and time. To fully unlock the spatio-temporal knowledge, we propose to decouple original inputs $\mathbf{X} \in \mathbb{R}^{N \times T \times C}$ into *temporal intrinsic signals* $\mathbf{X}_{int} \in \mathbb{R}^{N \times T \times C}$ and *spatial diffusive signals* $\mathbf{X}_{dif} \in \mathbb{R}^{N \times T \times C}$, denoted as $\mathbf{X} = \mathbf{X}_{int} + \mathbf{X}_{dif}$. Concretely, our spatio-temporal decoupling block consists of two key components: Fourier analysis and structural diffusion operator, which are introduced as follows.

Inspired by previous works [27, 42] that model the time series in Fourier space, we first decompose the input spatio-temporal data in the frequency space using Fourier analysis. By doing so, we disentangle temporal intrinsic signals and spatial diffusion signals from intricate spatio-temporal time series by Fourier analysis and structural diffusion operator. Specifically, we calculate the frequency representations $\tilde{\mathbf{X}} = \text{Fourier}(\mathbf{X})$ for all nodes in the look-back window of T steps and sort them based on the amplitude, where $\text{Fourier}(\cdot)$ denotes the Fast Fourier Transform (FFT) operator. We take the top percentage of ϵ as the high-frequency signals $\tilde{\mathbf{X}}_{high}$, which represent the local fluctuations that can be diffused to spatial neighbors. The remaining low-frequency signals $\tilde{\mathbf{X}}_{low}$ are the intrinsic signals along time dimension. The whole process can be formally defined as:

$$\tilde{\mathbf{X}}_{high} = f_h(\epsilon, \tilde{\mathbf{X}}), \quad \tilde{\mathbf{X}}_{low} = f_l(\epsilon, \tilde{\mathbf{X}}), \quad (2)$$

where $f_h(\cdot)$ and $f_l(\cdot)$ are the filters that only pass the specific spectrums above and below ϵ , respectively. Intuitively, the low-frequency signals preserve the intrinsic characteristics of each node, whereas the high-frequency signals implicitly reflect the information of other nodes obtained through spatial interactions, such as traffic congestion and air pollution diffusion. We extensively conduct experiments to verify the effectiveness of this decoupling method. To enrich the diffusion information, we explicitly propagate the high-frequency signals over space via a structural diffusion operator. Motivated by spectral graph convolution [47], we leverage the eigenvectors of the Laplacian matrix of the pre-defined spatial graph G , defined as

$$\mathbf{X}_{dif} = \text{Fourier}^{-1}(\mathbf{U}^\top \tilde{\mathbf{X}}_{high}), \quad (3)$$

$$\mathbf{X}_{int} = \text{Fourier}^{-1}(\tilde{\mathbf{X}}_{low}), \quad (4)$$

where \mathbf{U} represents the matrix of eigenvectors of the graph Laplacian matrix M_G performed as $\mathbf{M}_G = \mathbf{U}\Lambda\mathbf{U}^\top$, where Λ is the diagonal matrix of eigenvalues. The eigenvector matrix \mathbf{U} is used to diffuse the high-frequency signals $\tilde{\mathbf{X}}_{high}^i$ in the Fourier domain, resulting in a frequency domain representation that incorporates the graph structural information. Finally, we perform an inverse FFT $\text{Fourier}^{-1}(\cdot)$ on the low- and high-frequency components to convert them back to the time domain and replace the original \mathbf{X} by concatenating \mathbf{X}_{int} and \mathbf{X}_{dif} as $\mathbf{X}_{dec} = \mathbf{X}_{int} || \mathbf{X}_{dif} \in \mathbb{R}^{N \times T \times 2C}$. After Fourier analysis, we are able to effectively capture the underlying dynamics of the spatio-temporal data, which facilitates more precise modality alignment in semantic space.

Additionally, to enhance the information density of decoupled signals, we employ patching strategy [30, 44] to construct patches as the input tokens for PLMs. Given the decoupled signals \mathbf{X}_{dec} , we divide the time series of each node as a series of non-overlapped patches $\mathbf{X}_{dec}^P \in \mathbb{R}^{N \times P \times L_P \times 2C}$, where $P = [T/T_P] + 1$ represents the number of the resulting patches, and T_P denotes the patch length. Next, we encode the patched signals as patched embeddings $\mathbf{X}_{enc} \in \mathbb{R}^{N \times P \times D}$

$$\mathbf{X}_{enc} = \text{Conv}(\mathbf{X}_{dec}^P, \theta_p), \quad (5)$$

where N stands for the number of nodes, and D is the embedding dimension. $\text{Conv}(\cdot)$ denotes the patch-wise convolution operator using filters with 1×1 kernel size and θ_p represents the learnable parameters of the patch-wise convolution. Unlike previous works [23, 26] that simply regard each node as a token, our model treats each patch as one token, allowing to construct relationships among

patches. By doing so, our model can preserve fine-grained local semantic information, allowing a more comprehensive understanding of spatio-temporal data.

Differentiable Discrete Reprogramming. Existing approach [17] aligns time series data by using a compressed vocabulary of the whole vocabulary $\mathbf{E} \in \mathbb{R}^{V \times d}$ of the PLMs, where V is the vocabulary size and d is the dimension of the embedding. However, due to the complex dynamic spatio-temporal dependencies, the semantics of spatio-temporal data are usually richer than that of ordinary time series. Therefore, such a method may encounter information bottleneck. Besides, they adopt linear mapping to condense the vocabulary, which mixes and distorts the original word meanings, leading to imprecise reprogramming. We resolve these issues by sampling original word embeddings from the whole vocabulary \mathbf{E} discretely and adaptively, which retains unmixed semantic information and makes full use of the expressive vocabulary at the same time.

Given the whole vocabulary \mathbf{E} , we introduce a word mask vector $\mathbf{m} \in \mathbb{R}^{V \times 1}$ to select the most relevant words, where $\mathbf{m}[i] \in \{0, 1\}$. In specific, we first obtain \mathbf{m} through a linear layer followed by a Softmax activation, denoted as $\mathbf{m} = \text{Softmax}(\mathbf{E}\mathbf{W})$, where \mathbf{W} is a learnable matrix. Afterward, we sample Top-K word embeddings from \mathbf{E} based on probability $\mathbf{m}[i]$ associated with word i for reprogramming. Since the sampling process is non-differentiable, we employ Gumbel-Softmax trick [14] to enable gradient calculation with back-propagation, defined as

$$\mathbf{m}'[i] = \frac{\exp((\log \mathbf{m}[i] + g_i)/\tau)}{\sum_{j=1}^V \exp((\log \mathbf{m}[j] + g_j)/\tau)}, \quad (6)$$

where \mathbf{m}' is a continuous relaxation of binary mask vector \mathbf{m} for word selection, τ is temperature coefficient, g_i and g_j are i.i.d random variables sampled from distribution $\text{Gumbel}(0, 1)$. Concretely, the Gumbel distribution can be derived by first sampling $u \sim \text{Uniform}(0, 1)$ and then computing $g_i = -\log(-\log(u))$. By doing so, we can expand vocabulary space while preserving the semantic meaning of each word.

After obtaining the sampled word embeddings $\mathbf{E}' \in \mathbb{R}^{K \times d}$, we perform modality alignment by using cross-attention. In particular, we define the query matrix $\mathbf{X}_q = \mathbf{X}_{enc}\mathbf{W}_q$, key matrix $\mathbf{X}_k = \mathbf{E}'\mathbf{W}_k$ and value matrix $\mathbf{X}_v = \mathbf{E}'\mathbf{W}_v$, where \mathbf{W}_q , \mathbf{W}_k , and \mathbf{W}_v . After that, we calculate the reprogrammed patch embedding as follows

$$\mathbf{Z} = \text{Attn}(\mathbf{X}_q, \mathbf{X}_k, \mathbf{X}_v) = \text{Softmax}\left(\frac{\mathbf{X}_q \mathbf{X}_k^\top}{\sqrt{d}}\right) \mathbf{X}_v, \quad (7)$$

where $\mathbf{Z} \in \mathbb{R}^{N \times P \times d}$ denotes the aligned textual representations for the input spatio-temporal data.

3.2 Spatio-Temporal Predictor

Based on the aligned representation, we utilize the frozen PLMs as the backbone for further processing. Roughly, PLMs consist of three components: self-attention, Feedforward Neural Networks, and layer normalization layer, which contain most of the learned semantic knowledge from pre-training. The reprogrammed patch embedding \mathbf{Z} is encoded by this frozen language model to further process the semantic information and generates hidden textual representations \mathbf{Z}_{text} . A learnable mapping function is then used to generate the desired target outputs, which map the textual representations into feature prediction.

Overall, in our REPST, the process of predicting the future states $\hat{\mathbf{Y}}$ based on the history observation \mathbf{X} can be simply formulated as:

$$\mathbf{Z} = \text{De-Reprogramming}(\mathbf{X}, \mathbf{E}), \quad (8)$$

$$\mathbf{Z}_{text} = \text{PLM}(\mathbf{Z}), \quad (9)$$

$$\hat{\mathbf{Y}} = \text{Projection}(\mathbf{Z}_{text}), \quad (10)$$

where $\text{De-Reprogramming}(\cdot, \cdot)$ represents the decoupling-based spatio-temporal reprogramming block and $\text{PLM}(\cdot)$, $\text{Projection}(\cdot)$ is the frozen PLM and learnable mapping function.

Model Optimization. Following the previous GNN-based works [37, 32], our REPST aims to minimize the mean absolute error (MAE) between the predicted future states $\hat{\mathbf{Y}}$ and ground truth \mathbf{Y} .

This provides us effective capability to generate predictions among various spatio-temporal scenarios.

$$\mathcal{L} = \frac{1}{N} \sum_{i=1}^N \left| \hat{\mathbf{y}}^i - \mathbf{y}^i \right|, \quad (11)$$

Here, $\hat{\mathbf{y}}^i, \mathbf{y}^i$ represents a sample from $\hat{\mathbf{Y}}$ and \mathbf{Y} , and N represent the total number of samples.

Scalability. Technically, the proposed REPST can be viewed as utilizing GPT-2 after performing cross-attention over $N \times P$ patches and V' word embeddings, which has the time and memory complexities that scale with $\mathcal{O}(N \cdot P \cdot V' + (N \cdot P)^2)$. Notably, the frozen GPT-2 blocks account for $\mathcal{O}((N \cdot P)^2)$, which do not participate in back propagation. To reduce such computational burden that undermines the application of the proposed method to large N , we train the model by partitioning the pre-defined spatial graph into multiple sub-graphs. In practice, we train REPST by sampling a sub-graph each time. By doing so, we can effectively reduce the computational costs and enable the model to scale to large N .

4 Experiments

We thoroughly validate the effectiveness of REPST on various real-world datasets, including the overall forecasting performance, the few-shot generability, the ablation study, and the case study. We first introduce the experimental settings, including datasets and baselines. Then we conduct experiments to compare the overall performance and few-shot of our REPST with other previous works. Furthermore, we design comprehensive ablation studies to evaluate the impact of the essential architectures and components. Finally, we conduct case studies to analyze the performance qualitatively.

4.1 Experimental Settings

4.1.1 Datasets

We conducted experiments on four commonly used real-world datasets [34, 19], each varying in the fields of traffic, solar energy, and air quality. The traffic datasets, Beijing Taxi and NYC Bike, are collected every 30 minutes from hundreds of individual detectors spanning the freeway systems across all major metropolitan areas of Beijing and NYC. These datasets are extensively used in spatio-temporal forecasting studies due to their comprehensive coverage and detailed temporal resolution. The Air Quality¹ dataset includes six indicators (PM2.5, PM10, NO₂, CO, O₃, SO₂) to measure air quality, collected hourly from 35 stations across Beijing, providing a detailed temporal and spatial view of pollution levels. Lastly, the Solar Energy dataset records variations every 10 minutes from 137 photovoltaic (PV) plants across Alabama, capturing the dynamic changes in solar energy production across different locations and times. Each dataset comprises tens of thousands of time steps and hundreds of nodes, offering a robust foundation for evaluating spatio-temporal forecasting models. The statistics of the datasets are summarized in Appendix.

4.1.2 Baselines

We extensively compare our proposed REPST with the state-of-the-art forecasting approaches, including (1) the GNN-based methods: Graph Wavenet [37], D2STGNN [33] (2) non-GNN-based state-of-the-art models: STID [32] and STNorm [4] which emphasizes the integration of spatial and temporal identities; (3) PLM-based time series forecasting models: FPT [46]. We reproduce all of the baselines based on the original paper or official code.

4.2 Overall Performance of REPST

Table 1 reports the overall performance of our proposed REPST as well as baselines in 4 real-world datasets with the best in **bold** and the second underlined. As can be seen, REPST outperforms all baselines in all spatio-temporal forecasting settings.

¹https://www.biendata.xyz/competition/kdd_2018/data/

Table 1: Overall Performance on 4 Real-world Datasets

| Dataset | Solar Energy | | Air Quality | | Beijing Taxi | | NYC Bike | |
|--------------|--------------|-------------|--------------|--------------|--------------|--------------|-------------|-------------|
| Metric | MAE | RMSE | MAE | RMSE | MAE | RMSE | MAE | RMSE |
| GWNet | 3.55 | 5.39 | 31.57 | 44.82 | 15.69 | 26.82 | 5.94 | <u>9.92</u> |
| STNorm | 4.17 | 5.99 | 30.73 | 44.82 | <u>15.37</u> | 27.50 | 5.93 | 10.37 |
| D2STGNN | 4.36 | 5.85 | 27.77 | 41.87 | 24.33 | 45.65 | 7.51 | 13.64 |
| STID | 3.70 | 5.57 | <u>26.94</u> | <u>41.01</u> | 15.60 | 27.96 | <u>5.85</u> | 10.44 |
| STAEFormer | <u>3.44</u> | <u>5.21</u> | 28.12 | 41.83 | 15.47 | <u>26.45</u> | 5.86 | 9.98 |
| FPT | 6.02 | 8.31 | 28.65 | 43.55 | 32.41 | 55.28 | 9.31 | 14.14 |
| REPST | 3.27 | 5.12 | 26.20 | 39.37 | 15.13 | 25.44 | 5.75 | 9.86 |

Notably, REPST surpasses the state-of-the-art PLM-based time series forecaster FPT [46] by a large margin in spatio-temporal forecasting tasks, which can demonstrate that simply leveraging the PLMs cannot handle problems with complex spatial dependencies. The alignment of spatio-temporal data and textual representations plays an essential role in the excellent performance of our proposed model. Additionally, the performance of the impressive PLM-based time series forecaster FPT [46] is still ineffective in Solar Energy, Air Quality and traffic scenarios, indicating that PLM methods for time-series are inapplicable for spatio-temporal scenarios. Our spatio-temporal reprogramming block leverages a wide range of vocabulary and sample words that can adequately capture the spatio-temporal patterns, which do make an impact on unlocking the capabilities of PLMs to capture fine-grained spatio-temporal dynamics.

4.3 Few-shot Performance

PLMs are trained using large amounts of data that cover various fields, equipping them with cross-domain knowledge. Therefore, PLMs can utilize specific spatio-temporal related textual representations to unlock their capabilities for spatio-temporal reasoning, which can handle the difficulties caused by data sparsity. To verify this, we further conduct experiments on each field to evaluate the predictive performance of our proposed REPST in data-sparse scenarios. Our evaluation results are listed in Table 2. Concretely, all models are trained on 1-day data from the train datasets and tested on the whole test dataset. REPST consistently outperforms other deep models and PLM-based time series forecasters in various datasets. This illustrates that our REPST can perform well on a new downstream dataset and is suitable for spatio-temporal forecasting tasks with the problem of data sparsity.

Specifically, PLM-based forecaster FPT and our REPST show competitive performance over other deep model baselines in few-shot experiments. It demonstrates that PLMs contain a wealth of time series and spatio-temporal related knowledge from pre-training. Moreover, the capabilities of spatio-temporal reasoning can be enhanced by limited data. This shows a reliable performance when transferred to data-sparse scenarios.

Table 2: Few-shot Performance

| Datasets | Metric | GWNet | STNorm | STAEFormer | STID | D2STGNN | FPT | REPST |
|--------------|--------|-------|--------------|--------------|-------|--------------|--------------|--------------|
| Solar Energy | MAE | 9.10 | 9.36 | 9.36 | 10.33 | 8.80 | 10.59 | 7.27 |
| | RMSE | 11.87 | 12.74 | 12.57 | 13.87 | <u>11.26</u> | 13.92 | 9.98 |
| Air Quality | MAE | 36.26 | 36.38 | 37.68 | 43.21 | 40.77 | <u>35.62</u> | 33.57 |
| | RMSE | 54.88 | 57.66 | 53.39 | 61.07 | 55.07 | <u>51.33</u> | 47.30 |
| Beijing Taxi | MAE | 29.24 | 28.92 | <u>28.88</u> | 32.73 | 36.73 | 41.66 | 26.85 |
| | RMSE | 51.68 | 50.59 | <u>49.86</u> | 51.77 | 58.70 | 74.87 | 45.88 |
| NYC Bike | MAE | 12.55 | <u>11.69</u> | 12.50 | 12.31 | 12.70 | 13.47 | 9.66 |
| | RMSE | 21.97 | <u>20.17</u> | 20.77 | 21.37 | 21.81 | 23.26 | 17.45 |

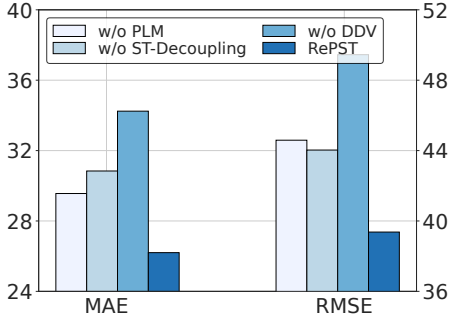


Figure 2: Air Quality

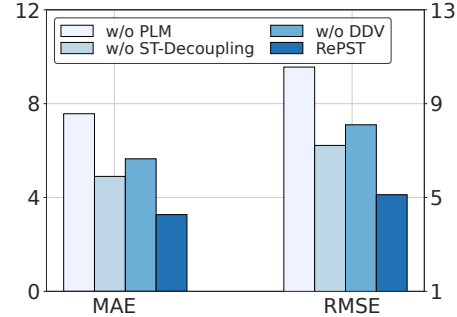


Figure 3: Solar Energy

Figure 4: Model Ablation

4.4 Ablation Study

To figure out the effectiveness of each component in our RePST, we further conduct detailed ablation studies on Solar Energy and Beijing Air Quality with three variants as follows:

- w/o Pre-trained Language Model backbone (PLM): it removes the pre-trained language model backbone.
- w/o Spatio-temporal Decoupling Block (ST-Decoupling): it removes the Spatio-temporal decoupling block.
- w/o Differentiable Discrete Reprogramming (DDR): it removes the discrete mapping vocabulary and utilizes the dense mapping function to decrease the vocabulary size.

Figure 4 shows the comparative performance of the variants above on Solar Energy and Air Quality. Based on the results, we can make the conclusions as follows: (1) The PLM benefits modeling relationships among patches, effectively constructing spatial dependencies by leveraging multi-head attention. (2) The spatio-temporal decoupling block which decomposes input spatio-temporal data into intrinsic signals and diffusive signals can actually enable PLMs to better understand different data compositions. This results in relieving the burden of modality alignment as well. (3) The impressive performance in w/o Differentiable Discrete Vocabulary demonstrates that leveraging the whole vocabulary and selecting relevant discrete textual information achieves accurate reprogramming which enables PLM to better understand the underlying spatio-temporal patterns.

5 Related Works

5.1 Pretrained Language Models for Time Series

Recently, Pretrained Language Models(PLMs) have shown outstanding performance on time series analysis tasks, including forecasting[46, 8, 43], classification[35], Anomaly Detection[46]. We have witnessed a large amount of effort in handling time series analysis tasks leveraging the power of PLMs [3, 46, 7, 20]. However, they fail to address the problem of the modality gap between time series and natural language. To solve this problem, Time-LLM[17] first utilizes reprogramming, which is an effective approach to handle the problem of modality gap. Its goal is to identify a trainable input data transformation function H that is applicable across all target input data, enabling the reprogramming of input data into the source data space. Examples include reprogramming an acoustic model to handle time series data [41].

However, Time-LLM [17] only maintains a small compressed vocabulary, which might not be expressive enough for encoding complex spatio-temporal patterns, which is essential for spatio-temporal forecasting. Additionally, in order to handle the problem of over-fitting, Time-LLM obtains a small vocabulary by mapping the whole vocabulary of PLMs densely. Unlike previous methods, we design a framework based on a spatio-temporal reprogramming block to cater to complicated challenges in spatio-temporal scenarios, which can make use of the whole vocabulary of PLMs while relieving the risk of over-fitting.

5.2 Spatio-Temporal Forecasting

Deep learning based spatio-temporal forecasting models have gained great focus these years due to their impressive performance in multiple fields, such as traffic flow [24, 32, 25], air quality[12, 11], electricity[6], etc [28, 39, 13]. Early deep learning approaches often employed GNN to process spatial information and attracted great attention. Spatio-temporal Neural Networks (STGNNs) utilize Graph Convolution Networks (GCNs) to model spatial dependencies by processing predefined graph structures and sequential models for temporal combination. For example, DCRNN [21] combines GCN with RNN and its variants. The static graph failed to reflect the complete spatial dependencies accurately, however, which may change with time. An increasing trend is to utilize adaptive spatio-temporal graph neural networks in order to capture the dynamic spatial dependencies. Graph WaveNet [37] proposes to learn a normalized adaptive adjacency matrix without a pre-defined graph. AGCRN [1] designs a Node Adaptive Parameter Learning enhanced layer to learn node-specific patterns. Additional, attention mechanisms are widely used in STGNNs, such as GMAN [45], STAEFormer [24] and ASTGNN [9]. Moreover, MLP-based STID [32] reaches the state-of-the-art performance on most of the spatio-temporal datasets by utilizing multiple embeddings.

Due to the exceptional generation capabilities of large language models, researchers are turning their attention to LLMs and considering the possibility of applying large language models to spatio-temporal data forecasting tasks. Several works [23, 26, 40, 15] explore the solution to leverage the Pre-trained language models to handle spatio-temporal tasks, among which, UrbanGPT [22] provides an elegant and performance-guaranteed end-to-end solution for spatio-temporal forecasting. It integrates spatio-temporal data with traditional textual information, enabling it to understand and predict urban dynamics. However, UrbanGPT does not explicitly align spatio-temporal information and natural language. This paper proposes a specially designed reprogramming block for spatio-temporal information and textual representations that can specifically align these two modalities.

6 Conclusion

In this paper, we explored the novel application of adopting Pre-trained Language Models (PLMs) for spatio-temporal forecasting by reprogramming spatio-temporal inputs into textual representations. To address the challenges in spatio-temporal modeling, we developed a spatio-temporal reprogramming block that decomposes input data into two types of spatio-temporal signals and transforms them into patches. These patches are then aligned textually using a differentiable discrete reprogramming strategy. The forecasting is made by a frozen GPT-2 backbone based on the reprogrammed patches. Extensive experiments demonstrate that our proposed framework, REPST, achieves state-of-the-art performance on real-world datasets and exhibits exceptional capabilities in few-shot scenarios.

References

- [1] Lei Bai, Lina Yao, Can Li, Xianzhi Wang, and Can Wang. Adaptive graph convolutional recurrent network for traffic forecasting. *Advances in neural information processing systems*, 33:17804–17815, 2020.
- [2] Shaojie Bai, J Zico Kolter, and Vladlen Koltun. An empirical evaluation of generic convolutional and recurrent networks for sequence modeling. *arXiv preprint arXiv:1803.01271*, 2018.
- [3] Defu Cao, Furong Jia, Sercan O Arik, Tomas Pfister, Yixiang Zheng, Wen Ye, and Yan Liu. Tempo: Prompt-based generative pre-trained transformer for time series forecasting. *arXiv preprint arXiv:2310.04948*, 2023.
- [4] Jinliang Deng, Xiusi Chen, Renhe Jiang, Xuan Song, and Ivor W Tsang. St-norm: Spatial and temporal normalization for multi-variate time series forecasting. In *Proceedings of the 27th ACM SIGKDD conference on knowledge discovery & data mining*, pages 269–278, 2021.
- [5] Jinliang Deng, Xiusi Chen, Renhe Jiang, Du Yin, Yi Yang, Xuan Song, and Ivor W Tsang. Disentangling structured components: Towards adaptive, interpretable and scalable time series forecasting. *IEEE Transactions on Knowledge and Data Engineering*, 2024.
- [6] Xu Geng, Yaguang Li, Leye Wang, Lingyu Zhang, Qiang Yang, Jieping Ye, and Yan Liu. Spatiotemporal multi-graph convolution network for ride-hailing demand forecasting. In

Proceedings of the AAAI conference on artificial intelligence, volume 33, pages 3656–3663, 2019.

- [7] Nate Gruver, Marc Finzi, Shikai Qiu, and Andrew G Wilson. Large language models are zero-shot time series forecasters. In A. Oh, T. Naumann, A. Globerson, K. Saenko, M. Hardt, and S. Levine, editors, *Advances in Neural Information Processing Systems*, volume 36, pages 19622–19635. Curran Associates, Inc., 2023.
- [8] Nate Gruver, Marc Finzi, Shikai Qiu, and Andrew G Wilson. Large language models are zero-shot time series forecasters. *Advances in Neural Information Processing Systems*, 36, 2024.
- [9] Shengnan Guo, Youfang Lin, Huaiyu Wan, Xiucheng Li, and Gao Cong. Learning dynamics and heterogeneity of spatial-temporal graph data for traffic forecasting. *IEEE Transactions on Knowledge and Data Engineering*, 34(11):5415–5428, 2021.
- [10] Wes Gurnee and Max Tegmark. Language models represent space and time. In *The Twelfth International Conference on Learning Representations*, 2023.
- [11] Jindong Han, Hao Liu, Hengshu Zhu, Hui Xiong, and Dejing Dou. Joint air quality and weather prediction based on multi-adversarial spatiotemporal networks. In *Proceedings of the AAAI Conference on Artificial Intelligence*, volume 35, pages 4081–4089, 2021.
- [12] Jindong Han, Weijia Zhang, Hao Liu, and Hui Xiong. Machine learning for urban air quality analytics: A survey. *arXiv preprint arXiv:2310.09620*, 2023.
- [13] Bing He, Dian Zhang, Siyuan Liu, Hao Liu, Dawei Han, and Lionel M Ni. Profiling driver behavior for personalized insurance pricing and maximal profit. In *2018 IEEE International Conference on Big Data (Big Data)*, pages 1387–1396. IEEE, 2018.
- [14] Eric Jang, Shixiang Gu, and Ben Poole. Categorical reparameterization with gumbel-softmax. *arXiv preprint arXiv:1611.01144*, 2016.
- [15] Wenzhao Jiang, Jindong Han, Hao Liu, Tao Tao, Naiqiang Tan, and Hui Xiong. Interpretable cascading mixture-of-experts for urban traffic congestion prediction. *arXiv preprint arXiv:2406.12923*, 2024.
- [16] Guangyin Jin, Yuxuan Liang, Yuchen Fang, Zezhi Shao, Jincai Huang, Junbo Zhang, and Yu Zheng. Spatio-temporal graph neural networks for predictive learning in urban computing: A survey. *IEEE Transactions on Knowledge and Data Engineering*, 2023.
- [17] Ming Jin, Shiyu Wang, Lintao Ma, Zhixuan Chu, James Y Zhang, Xiaoming Shi, Pin-Yu Chen, Yuxuan Liang, Yuan-Fang Li, Shirui Pan, et al. Time-lm: Time series forecasting by reprogramming large language models. *arXiv preprint arXiv:2310.01728*, 2023.
- [18] Ming Jin, Yifan Zhang, Wei Chen, Kexin Zhang, Yuxuan Liang, Bin Yang, Jindong Wang, Shirui Pan, and Qingsong Wen. Position paper: What can large language models tell us about time series analysis. *arXiv preprint arXiv:2402.02713*, 2024.
- [19] Guokun Lai, Wei-Cheng Chang, Yiming Yang, and Hanxiao Liu. Modeling long-and short-term temporal patterns with deep neural networks. In *The 41st international ACM SIGIR conference on research & development in information retrieval*, pages 95–104, 2018.
- [20] Siqi Lai, Zhao Xu, Weijia Zhang, Hao Liu, and Hui Xiong. Large language models as traffic signal control agents: Capacity and opportunity. *CoRR*, abs/2312.16044, 2023.
- [21] Yaguang Li, Rose Yu, Cyrus Shahabi, and Yan Liu. Diffusion convolutional recurrent neural network: Data-driven traffic forecasting. In *International Conference on Learning Representations*, 2018.
- [22] Zhonghang Li, Lianghao Xia, Jiabin Tang, Yong Xu, Lei Shi, Long Xia, Dawei Yin, and Chao Huang. Urbangpt: Spatio-temporal large language models. *arXiv preprint arXiv:2403.00813*, 2024.
- [23] Chenxi Liu, Sun Yang, Qianxiong Xu, Zhishuai Li, Cheng Long, Ziyue Li, and Rui Zhao. Spatial-temporal large language model for traffic prediction. *arXiv preprint arXiv:2401.10134*, 2024.
- [24] Hangchen Liu, Zheng Dong, Renhe Jiang, Jiewen Deng, Jinliang Deng, Quanjun Chen, and Xuan Song. Spatio-temporal adaptive embedding makes vanilla transformer sota for traffic forecasting. In *Proceedings of the 32nd ACM international conference on information and knowledge management*, pages 4125–4129, 2023.

[25] Hao Liu, Ying Li, Yanjie Fu, Huaibo Mei, Jingbo Zhou, Xu Ma, and Hui Xiong. Polestar: An intelligent, efficient and national-wide public transportation routing engine. In *Proceedings of the 26th ACM SIGKDD International Conference on Knowledge Discovery & Data Mining*, pages 2321–2329, 2020.

[26] Lei Liu, Shuo Yu, Runze Wang, Zhenxun Ma, and Yanming Shen. How can large language models understand spatial-temporal data? *arXiv preprint arXiv:2401.14192*, 2024.

[27] Yong Liu, Chenyu Li, Jianmin Wang, and Mingsheng Long. Koopa: Learning non-stationary time series dynamics with koopman predictors. *Advances in Neural Information Processing Systems*, 36, 2024.

[28] Hui Luo, Jingbo Zhou, Zhifeng Bao, Shuangli Li, J Shane Culpepper, Haochao Ying, Hao Liu, and Hui Xiong. Spatial object recommendation with hints: When spatial granularity matters. In *Proceedings of the 43rd International ACM SIGIR Conference on research and development in information retrieval*, pages 781–790, 2020.

[29] Gengchen Mai, Weiming Huang, Jin Sun, Suhang Song, Deepak Mishra, Ninghao Liu, Song Gao, Tianming Liu, Gao Cong, Yingjie Hu, et al. On the opportunities and challenges of foundation models for geospatial artificial intelligence. *arXiv preprint arXiv:2304.06798*, 2023.

[30] Yuqi Nie, Nam H Nguyen, Phanwadee Sinthong, and Jayant Kalagnanam. A time series is worth 64 words: Long-term forecasting with transformers. *arXiv preprint arXiv:2211.14730*, 2022.

[31] Zezhi Shao, Fei Wang, Yongjun Xu, Wei Wei, Chengqing Yu, Zhao Zhang, Di Yao, Guangyin Jin, Xin Cao, Gao Cong, et al. Exploring progress in multivariate time series forecasting: Comprehensive benchmarking and heterogeneity analysis. *arXiv preprint arXiv:2310.06119*, 2023.

[32] Zezhi Shao, Zhao Zhang, Fei Wang, Wei Wei, and Yongjun Xu. Spatial-temporal identity: A simple yet effective baseline for multivariate time series forecasting. In *Proceedings of the 31st ACM International Conference on Information & Knowledge Management*, pages 4454–4458, 2022.

[33] Zezhi Shao, Zhao Zhang, Wei Wei, Fei Wang, Yongjun Xu, Xin Cao, and Christian S Jensen. Decoupled dynamic spatial-temporal graph neural network for traffic forecasting. *arXiv preprint arXiv:2206.09112*, 2022.

[34] Chao Song, Youfang Lin, Shengnan Guo, and Huaiyu Wan. Spatial-temporal synchronous graph convolutional networks: A new framework for spatial-temporal network data forecasting. In *Proceedings of the AAAI conference on artificial intelligence*, volume 34, pages 914–921, 2020.

[35] Chenxi Sun, Yaliang Li, Hongyan Li, and Shenda Hong. Test: Text prototype aligned embedding to activate llm’s ability for time series. *arXiv preprint arXiv:2308.08241*, 2023.

[36] Hugo Touvron, Thibaut Lavril, Gautier Izacard, Xavier Martinet, Marie-Anne Lachaux, Timothée Lacroix, Baptiste Rozière, Naman Goyal, Eric Hambro, Faisal Azhar, et al. Llama: Open and efficient foundation language models. corr, abs/2302.13971, 2023. doi: 10.48550. *arXiv preprint arXiv:2302.13971*, 2023.

[37] Zonghan Wu, Shirui Pan, Guodong Long, Jing Jiang, and Chengqi Zhang. Graph wavenet for deep spatial-temporal graph modeling. *arXiv preprint arXiv:1906.00121*, 2019.

[38] Peng Xie, Tianrui Li, Jia Liu, Shengdong Du, Xin Yang, and Junbo Zhang. Urban flow prediction from spatiotemporal data using machine learning: A survey. *Information Fusion*, 59:1–12, 2020.

[39] Haoran Xin, Xinjiang Lu, Tong Xu, Hao Liu, Jingjing Gu, Dejing Dou, and Hui Xiong. Out-of-town recommendation with travel intention modeling. In *Proceedings of the AAAI Conference on Artificial Intelligence*, volume 35, pages 4529–4536, 2021.

[40] Yibo Yan, Haomin Wen, Siru Zhong, Wei Chen, Haodong Chen, Qingsong Wen, Roger Zimmermann, and Yuxuan Liang. When urban region profiling meets large language models. *arXiv preprint arXiv:2310.18340*, 2023.

[41] Chao-Han Huck Yang, Yun-Yun Tsai, and Pin-Yu Chen. Voice2series: Reprogramming acoustic models for time series classification. In *International conference on machine learning*, pages 11808–11819. PMLR, 2021.

- [42] Kun Yi, Qi Zhang, Wei Fan, Hui He, Liang Hu, Pengyang Wang, Ning An, Longbing Cao, and Zhendong Niu. Fourierggn: Rethinking multivariate time series forecasting from a pure graph perspective. *Advances in Neural Information Processing Systems*, 36, 2024.
- [43] Weijia Zhang, Chenlong Yin, Hao Liu, and Hui Xiong. Unleash the power of pre-trained language models for irregularly sampled time series. *arXiv preprint arXiv:2408.08328*, 2024.
- [44] Weijia Zhang, Chenlong Yin, Hao Liu, Xiaofang Zhou, and Hui Xiong. Irregular multivariate time series forecasting: A transformable patching graph neural networks approach. In *Forty-first International Conference on Machine Learning*, 2024.
- [45] Chuanpan Zheng, Xiaoliang Fan, Cheng Wang, and Jianzhong Qi. Gman: A graph multi-attention network for traffic prediction. In *Proceedings of the AAAI conference on artificial intelligence*, volume 34, pages 1234–1241, 2020.
- [46] Tian Zhou, Peisong Niu, Liang Sun, Rong Jin, et al. One fits all: Power general time series analysis by pretrained lm. *Advances in neural information processing systems*, 36, 2024.
- [47] Hao Zhu and Piotr Koniusz. Simple spectral graph convolution. In *International conference on learning representations*, 2020.

A Implementation Details

A.1 Baseline Models

- **D2STGNN:** D2STGNN [33] is an advanced model designed to improve the accuracy and efficiency of traffic prediction by addressing the complexities inherent in spatial-temporal data. By decoupling spatial and temporal components, the model reduces complexity, making it more computationally efficient without sacrificing accuracy.
- **STAEFormer:** STAEFormer is a cutting-edge model that elevates the standard Transformer architecture for traffic forecasting by incorporating Spatio-Temporal Adaptive Embeddings. These embeddings dynamically encode both spatial and temporal dependencies, allowing the model to capture the complex, evolving patterns typical in traffic data. The spatial embeddings represent geographical relationships between traffic nodes, while the temporal embeddings account for time-related patterns like rush hours or seasonal variations. Unlike traditional static embeddings, it adaptively adjusts to the changing traffic conditions, enhancing the model’s ability to predict future traffic flows with greater accuracy.
- **STNorm:** STNorm [4] normalizes data to better capture underlying patterns in both spatial and temporal dimensions. By addressing the variability in data across different time steps and locations, STNorm improves the accuracy of predictions, offering a robust approach to handling complex, dynamic datasets.
- **STID:** STID [32] emphasizes the integration of spatial and temporal identities to enhance predictive performance. It employs unique identifiers for spatial and temporal components to effectively capture and utilize the inherent structure and patterns in the data.
- **FPT:** FPT [46] demonstrate that partly frozen pre-trained models on natural language or images can handle all main time series analysis tasks.

A.2 Dataset Descriptions

We follow the same data processing and train-validation-test set split protocol used in the baseline models, where the train, validation, and test datasets are strictly divided according to chronological order to make sure there are no data leakage issues. As for the forecasting settings, we fix the length of the lookback series as 24, and the prediction length is 24. Four commonly used real-world datasets vary in fields of traffic (Beijing Taxi, NYC Bike), solar-energy and air quality (Air Quality), each of which holds tens of thousands of time steps and hundreds of nodes. Beijing Taxi and NYC Bike datasets are collected in every 30 minutes from nearly 40,000 individual detectors spanning the freeway system across all major metropolitan areas of NYC and Beijing, which are widely used in previous spatio-temporal forecasting studies. Air Quality dataset holds 6 indicators ($PM2.5$, $PM10$, NO_2 , CO , O_3 , SO_2) to measure air quality. They are collected from 35 stations in every 1 hour. And solar-energy dataset collect the every 10 minutes variations of 137 PV plants across Alabama. Notably, we construct the graph for 35 stations by leveraging the time series similarity between nodes. The details of datasets are provided in Table 3

Table 3: Detailed dataset descriptions. *Dim* denotes the variate number of each dataset. *Dataset Size* denotes the total number of time points in (Train, Validation, Test) split respectively. *Frequency* denotes the sampling interval of time points.

| Dataset | Dim | Dataset Size | Frequency | Information |
|--------------|------|----------------------|-----------|----------------|
| Air Quality | 35 | (6075, 867, 1736) | 1 hour | Air Quality |
| Beijing Taxi | 1024 | (3298, 1100, 1099) | 30 min | Transportation |
| NYC Bike | 128 | (2621, 874, 874) | 30 min | Transportation |
| Solar Energy | 137 | (36776, 5254, 10507) | 10 min | Energy |

A.3 Evaluation Metrics

Three metrics are used for evaluating the models: mean absolute error (MAE), mean absolute percentage error (MAPE) and root mean squared error (RMSE). Lower values of metrics stand for

better performance. RMSE and MAE measure absolute errors, while MAPE measures relative errors.

$$\begin{aligned} \text{MAE} &= \frac{1}{N} \sum_{i=1}^N \left| \hat{\mathbf{y}}^i - \mathbf{y}^i \right|, \\ \text{RMSE} &= \sqrt{\frac{1}{N} \sum_{i=1}^N (\hat{\mathbf{y}}^i - \mathbf{y}^i)^2}, \\ \text{MAPE} &= \frac{100\%}{N} \sum_{i=1}^N \left| \frac{\hat{\mathbf{y}}^i - \mathbf{y}^i}{\mathbf{y}^i} \right|, \end{aligned}$$

where $\hat{\mathbf{y}}^i, \mathbf{y}^i$ represents a sample from $\hat{\mathbf{Y}}$ and \mathbf{Y} , and N represent the total number of samples.

A.4 Implementation Details

Algorithm 1: REPST -Overall Architecture

Input: history observation \mathbf{X} , pre-defined spatial graph G , Fourier boundary ϵ , patch length L_P .
Result: predictive future states $\hat{\mathbf{Y}}$.

/* Step 1: Spatio-Temporal Decoupling */

- 1 Decouple the spatio-temporal input into high-frequency signals and low-frequency signals by Equations: $\tilde{\mathbf{X}}_{high} = f_h(\epsilon, \tilde{\mathbf{X}})$, $\tilde{\mathbf{X}}_{low} = f_l(\epsilon, \tilde{\mathbf{X}})$;
- 2 Obtain spatial diffusion signals by diffusing high-frequency signals in spatial space by Equation: $\mathbf{X}_{dif} = \text{Fourier}^{-1}(\mathbf{U}^\top \tilde{\mathbf{X}}_{high})$;
- 3 Obtain temporal intrinsic signals by: $\mathbf{X}_{int} = \text{Fourier}^{-1}(\tilde{\mathbf{X}}_{low})$;
- 4 Divide series in each node into patches;
- 5 Encode the patches as \mathbf{X}_{enc} by convolution operator: $\mathbf{X}_{enc} = \text{Conv}(\mathbf{X}_{dec}, \theta_p)$;

/* Step 2: Differentiable Discrete Reprogramming */

- 6 Initialize learnable vocabulary mask $m = \text{Gumbel_Softmax}(\mathbf{E}^\top \mathbf{W})$;
- 7 Obtain the sampled word embedding $\mathbf{E}' = \text{mask}(m, \mathbf{E})$;
- 8 Reprogramming the spatio-temporal embedding into textual representations \mathbf{Z} by Equation 7;
- 9 Encode by PLMs: $\mathbf{Z}_{text} = \text{PLM}(\mathbf{Z})$;
- 10 Generate final prediction by linear mapping function: $\hat{\mathbf{Y}} = \text{Projection}(\mathbf{Z}_{text})$;
- 11 Return predictive future states $\hat{\mathbf{Y}}$.

B Show Cases

To provide the visualization of the prediction effect, we list the prediction showcases of certain nodes contained in dataset Solar Energy. Concretely, we visualize the prediction and ground in 326 time steps of four nodes from the node set.

C Experimental Details

C.1 Hyper Parameter Settings

For our prediction tasks, we aim to predict the next 12 steps of data based on the previous 12 steps. Both the historical length (T) and prediction length (τ) are set to 12. Moreover, the parameters for the convolution kernel in patch embedding layers are set to 3 and the number of the multi-head attention layers of reprogramming layer is set to 1. Additionally, we obtain the embedding of patches with the dimension of 64.

C.2 Further Experimental Setup Descriptions

During the reprogramming phrase, we sample 1000 most relevant words to capture the complex dynamic spatio-temporal dependencies. It is important to note that the missing data of the training

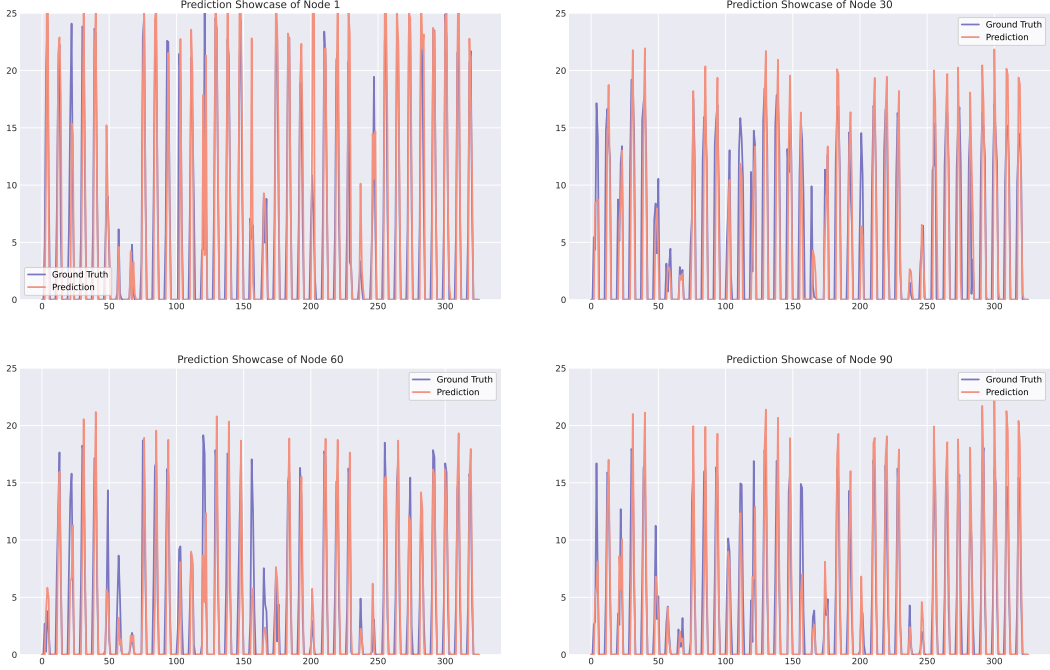


Figure 5: Showcases of Solar Energy

dataset are filled by the former time step of the same node. By doing so, it helps to improve the performance of pre-trained language models to handle spatio-temporal time series tasks. Because the value 0 could disturb the capabilities of pre-trained language models for understanding the consistent textual series. Similar to traditional experimental settings, each time series is split into three parts: training data, validation data, and test data. For the few-shot forecasting task, only a certain percentage timesteps of training data are used, and the other two parts remain unchanged. The evaluation metrics remain the same as for classic spatio-temporal time series forecasting. We repeat this experiment 3 times and report the average metrics in the following experiments. Additionally, before the training procedure, the Fourier representations of each node are pre-calculated to save reduce the computation cost, as a result of which to reduce the training time cost. All the experiments are implemented in PyTorch and conducted on a single NVIDIA RTX 3090 24GB GPU. We utilize ADAM with an initial learning rate of 0.002 and MAE loss for the model optimization. We set the number of frozen GPT-2 blocks in our proposed model $gpt_layers \in \{3, 6, 9, 12\}$. The dimension of patched representations D is set from $\{64, 128, 256\}$. All the compared baseline models that we reproduced are implemented based on the benchmark of BasicTS [31], which is developed based on EasyTorch, an easy-to-use and powerful open-source neural network training framework.

D Broader Impact

D.1 Impact on Real-world Applications

Our work copes with real-world spatio-temporal forecasting, which is faced with problems of data sparsity and intrinsic non-stationarity that poses challenges for deep models to train a domain foundation model. Since previous works thoroughly explore the solutions to deal with various spatio-temporal dependencies, we propose a novel approach which leverage the power of pre-trained language models to handle spatio-temporal forecasting tasks, which fundamentally considers the natural connection between spatio-temporal information and natural language and achieves modality alignment by leveraging reprogramming. Without additional effort on prompts engineering [22, 40] which is a time-cost but essential part in enhancing the capabilities of pre-trained language models, our REPST automatically learns the spatio-temporal related vocabulary which can unlock the domain knowledge of pre-trained language models to do spatio-temporal reasoning and predictive generation.

Our model reaches state-of-the-art performance on the four real-world datasets , covering energy, air quality and transportation, and demonstrates remarkable capability to handle problem of data sparsity. Therefore, the proposed model makes it promising to tackle real-world forecasting applications, which can help our society to prevent multiple risks in advance with limited computational cost and small amount of data.

D.2 Impact on Future Research

In this paper, we find that models trained on natural languages can handle spatio-temporal forecasting tasks, which is totally a different data modality from natural language. This demonstrates that aligning different data modality properly can unlock the domain knowledge obtained by the pre-trained model during the training process. Therefore, there is a possibility that models that pre-trained on data from various domains hold the capability to handle problems in different fields even if in different modalities. The underlying reasons why pre-trained models can handle cross-modality tasks still remains to be explain.

E Limitation

Our proposed model does not respectively consider the optimization of computational complexity. Due to the large amount of parameters obtained by pre-trained language models, it costs more time to train the model compared to other deep learning based models. Although training models by partitioning the per-defined spatial graph and keeping PLMs frozen can relieve, the problem of scalability stills plagues in our work. Therefore, methods for modality alignment between spatio-temporal information and textual representations which aim at computational efficiency can be promising for spatio-temporal forecasting with pre-trained language models, which leaves our future work.